Baltic Astronomy, vol. 24, 223–230, 2015

STOCHASTIC 2-D GALAXY DISK EVOLUTION MODELS. RESOLVED STELLAR POPULATIONS IN THE GALAXY M33

T. Mineikis[1,2] and V. Vansevičius[1,2]

[1] *Vilnius University Observatory, Čiurlionio 29, Vilnius LT-03100, Lithuania; vladas.vansevicius@ff.vu.lt*

[2] *Center for Physical Sciences and Technology, Savanorių 231, Vilnius LT-02300, Lithuania; tadas.mineikis@ftmc.lt*

Received: 2015 June 04; accepted: 2015 July 14

Abstract. We improved the stochastic 2-D galaxy disk models (Mineikis & Vansevičius 2014a) by introducing enriched gas outflows from galaxies and synthetic color-magnitude diagrams of stellar populations. To test the models, we use the HST/ACS stellar photometry data in four fields located along the major axis of the galaxy M33 (Williams et al. 2009) and demonstrate the potential of the models to derive 2-D star formation histories in the resolved disk galaxies.

Key words: galaxies: evolution – galaxies: individual (M33)

1. INTRODUCTION

One of the most informative sources to study the evolution of galaxy disks is a resolved stellar photometry. Accurate photometric data supported by realistic galaxy evolution models allow one to derive the most important galaxy parameters – star formation (SF) and metal enrichment histories, see, e.g., Aparicio & Hidalgo (2009). Moreover, the possibility of determining 2-D star formation (SF) histories over wide areas offers perhaps the best opportunity to peer into large scale (beyond giant molecular clouds) SF processes in the galaxy disks.

Recent studies based on wide field and deep stellar photometry data in nearby galaxies revealed spatially resolved SF histories, see, e.g., Harris & Zaritsky (2009), Rubele et al. (2015), Lewis et al. (2015). Such studies, focussing on the large scale SF in galaxies, could lead to better understanding of the SF processes in general. For this purpose the 2-D stochastic galaxy disk evolution models (Mineikis & Vansevičius 2014a) could serve as an alternative to the widely employed, however, computationally expensive hydrodynamical models.

In this paper, we extend further our study of the galaxy M33 (Mineikis & Vansevičius 2014a) using improved 2-D stochastic galaxy disk models. The models are improved in two aspects: outflows of the enriched gas are considered and capabilities to generate synthetic stellar photometry catalogs are implemented. These new features enhanced the models and made them useful for the analysis of spatially resolved SF histories in disk galaxies.

2. THE MODELS

In this section we only briefly sketch our 2-D galaxy disk models, which are presented in Mineikis & Vansevičius (2014a) and compared with 1-D cases in Mineikis & Vansevičius (2014b). Below we discuss in more detail only new features implemented in the models recently: a prescription of gas outflows from galaxies and a method of synthetic stellar photometry data generation.

2.1. 2-D galaxy disk models

The 2-D galaxy disk models are composed of concentric rings subdivided into cells of equal area. The disk mass is building up by a gradual gas accretion from the reservoir where gas resides initially. The accretion rate follows a mean dark matter accretion rate as reported by Fakhouri, Ma & Boylan-Kolchin (2010). The SF is simulated by stochastic SF events in the model cells. The main model parameters determining stochastic SF are the probability of triggered SF, $P_{\rm T}$, and the SF efficiency (SFE). $P_{\rm T}$ controls the intensity of propagating SF. SFE depends on the average gas density in bursting cells, $\Sigma_{\rm G}$, and two parameters, ϵ and α:

$$\mathrm{SFE} = \epsilon \cdot \left(\frac{\Sigma_{\rm G}}{10\, M_\odot/\mathrm{pc}^2} \right)^{\alpha}. \tag{1}$$

2.2. Gas outflows

In the previous study (Mineikis & Vansevičius 2014a) we introduced gas flows between the cells, occurring due to SF events in the neighboring cells. In this study we consider, in addition, the case when a fraction of gas residing in a cell is ejected during the SF event and leaves the galaxy.

We implemented a model of expanding super-bubbles in stratified atmospheres following Baumgartner & Breitschwerdt (2013). We assume that, after the SF event in a cell, all newly formed supernovae explode in the center of the cell, which is located exactly at the mid-plane of the disk. We derive the mid-plane gas density assuming the conditions of hydrostatic equilibrium and a constant, along disk radius, scale height, $h_z = 100\,\mathrm{pc}$. These approximations make the speed of the expanding super-bubble in the z direction (perpendicular to the galaxy disk) dependant only on the gas density in the cell and the mass of newly formed stars (luminosity of the last stellar population).

Baumgartner & Breitschwerdt (2013) derived the conditions for disk gas outflow for the Milky Way by assuming that the expansion velocity of the top of super-bubble reaches a critical value, $v_{z,\mathrm{c}} = 20\,\mathrm{km\,s^{-1}}$, before the acceleration (due to the exponential drop in gas density) in the z direction begins. We applied the same critical value to our models of the galaxy M33.

In our models we assume that, once the outflow condition is fulfilled for the SF event, the cell loses gas instantly. We also assume that the gas lost from the cell is composed of the ejecta produced during the last 10 Myr from dying stars of all populations residing in it. Therefore, the mass of gas lost from the cell i, $m_{\mathrm{OUT},i}$, after the SF event is:

$$m_{\mathrm{OUT},i} = \begin{cases} 0, & n_{\rm SN} \le f(\Sigma_{\mathrm{G},i}) \\ \eta \cdot F_i, & n_{\rm SN} > f(\Sigma_{\mathrm{G},i}), \end{cases} \tag{2}$$

where $n_{\rm SN}$ is an average number of supernovae expected from the SF event, $f(\Sigma_{\mathrm{G},i})$

Table 1. The parameters used to generate synthetic CMDs.

Parameter	Description	Reference
Isochrone library	Parsec 1.2S	Bressan et al. (2012), Chen et al. (2014), Tang et al. (2014)
Mass loss on RGB	$\eta_{\rm Reimers} = 0.2$	default value
Initial mass function	corrected for binaries	Kroupa (2002)

denotes the Baumgartner & Breitschwerdt (2013) condition for the outflow, F_i is a fraction of gas returned during the last 10 Myr from all populations residing in the cell, and η is a free parameter controlling the fraction of the lost gas. If the SF event produces $n_{\rm SN} \leq 2$, the outflow from the cell is suppressed.

2.3. CMDs generation

For each disk model cell we keep a complete star formation history in a matrix $S(t, Z)$ with age t and metallicity Z dimensions. The step in age dimension, δt, is equal to the model integration time step. The step in metallicity dimension varies in the range 0.1−0.3 dex. Each stellar population, corresponding to the particular matrix element, at birth is generated by using a stochastically sampled initial mass function (IMF). We assume that stellar population j, corresponding to the matrix element $S(t_j, Z_j)$, has ages uniformly sampled within the time interval δt. For each stellar population j, we find in the library the nearest by age isochrone and interpolate the luminosity for each star of this population. However, we do not interpolate stellar luminosities between metallicities. See Table 1 for the parameters used to generate CMDs.

2.4. Model parameters

We use the same set-up of the model grid as in Mineikis & Vansevičius (2014a). Taking into account that gas outflows, implemented in the models, remove only enriched gas, the strongest effect is expected on the evolution of galaxy's metallicity. Since the enriched gas makes up a small fraction of the total mass of a galaxy, its removal can have only a negligible effect on the galaxy's total mass budget.

For the present study we used three models possessing the following values of parameters $P_{\rm T}$ and ϵ along the "degeneracy valley" (Mineikis & Vansevičius 2014a): 0.3 and 1.0% (the model A), 0.34 and 0.2% (the model B), and 0.44 and 0.1% (the model C), respectively. For simplicity, we kept the parameter α fixed at the value $\alpha = 2$ and generated three corresponding sets of models by varying the outflow parameter η in the range 0.2-0.9.

3. RESULTS

A comparison of the updated stochastic 2-D galaxy disk models with the observational data for the galaxy M33 is presented in Fig. 1, where the radial profiles of gas surface density, surface brightness in the i and FUV passbands, and metallicity are shown. The observed radial profiles of surface brightness are de-projected by adopting 54° for the inclination of the galaxy's disk. In the models, metallicity is converted to the oxygen abundance, with the solar metallicity, $Z_{\odot} = 0.015$ (Bressan et al. 2012), and the solar oxygen abundance of 8.67 (Asplund et al.

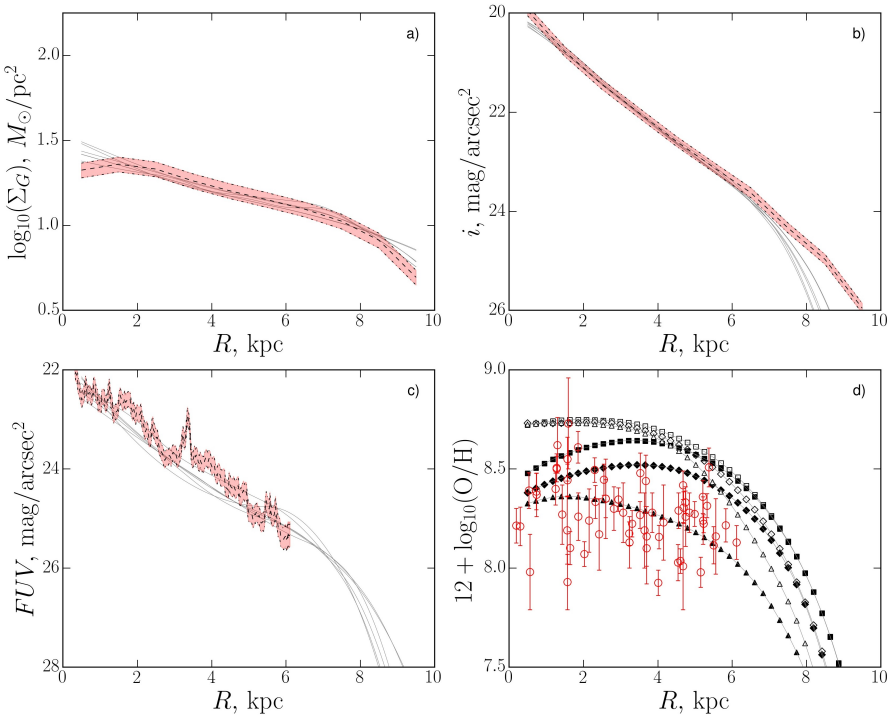

Fig. 1. Comparison of the observation data for the galaxy M33 with models: a) radial profiles of the gas surface density obtained by co-adding H I (Corbelli & Salucci 2000) and H_2 (Heyer et al. 2004) gas surface density profiles; b) radial profiles of the surface brightness in the i passband (Ferguson et al. 2007) deprojected to face-on and corrected for internal extinction using the radial extinction profile (Munoz-Mateos et al. 2007) and assuming the LMC type extinction law (Gordon et al. 2003); c) radial profiles of the surface brightness in the GALEX FUV passband (Munoz-Mateos et al. 2007) deprojected to face-on and corrected for internal extinction; d) radial profiles of oxygen abundance of HII zones by Rosolowsky & Simon (2008) (empty circles with error bars) and model oxygen abundance (triangles – $P_T = 0.3$ and $\epsilon = 1\%$, diamonds – $P_T = 0.34$ and $\epsilon = 0.2\%$, squares – $P_T = 0.44$ and $\epsilon = 0.1\%$; open symbols correspond to $\eta = 0.2$, filled symbols to $\eta = 0.9$).

2009).

The new models produce "degeneracy valley" almost identical to that demonstrated in Mineikis & Vansevičius (2014a). The only significant difference is seen in the metallicity radial profiles, because the model galaxies lose different amount of metal enriched gas due to different SF efficiency along the "degeneracy valley". The models with the highest ϵ values experience more massive SF events which are capable of producing outflows even in the outer disk regions. In contrast, the models with the lowest ϵ values form less massive stellar populations, i.e., cells lose a smaller amount of the enriched gas. The radial profiles of the enriched gas loss also differ between the models. In the central parts of the galaxy, all models lose a similar fraction of the enriched gas, however, in the outer parts the difference becomes more pronounced. The models with highest values of ϵ lose significantly more metals in the outer parts compared to the lowest ϵ models. Therefore, the

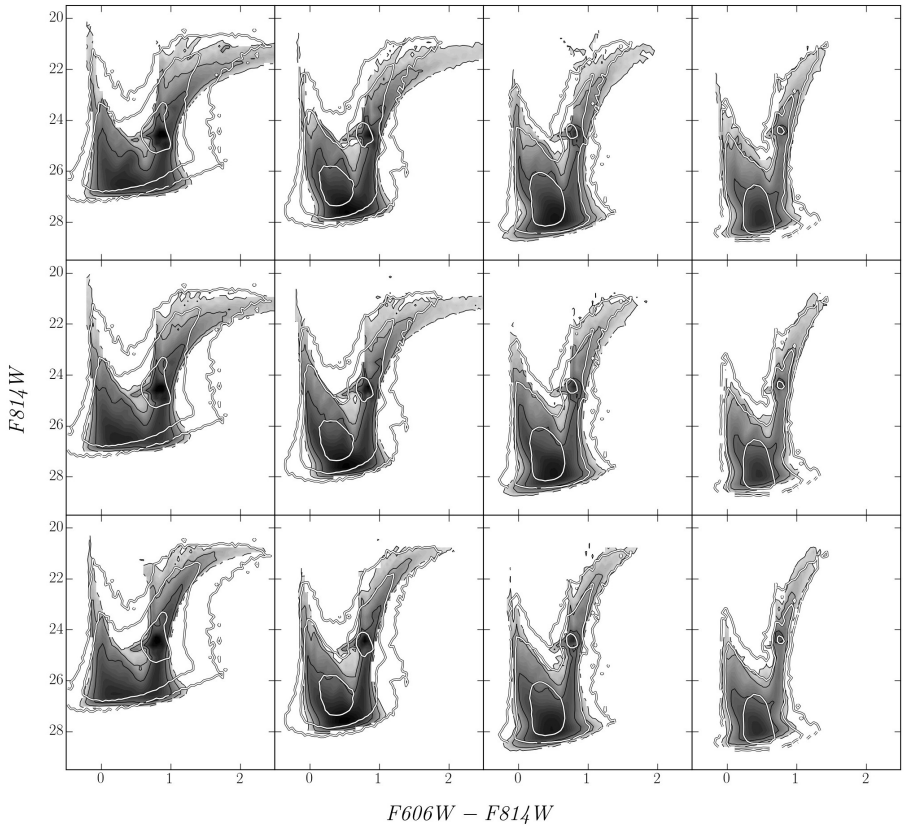

Fig. 2. HST/ACS WFC resolved stellar photometry data of the galaxy M33 (Williams et al. 2009). The contour lines represent the observed CMD star density on the logarithmic scale (adjacent lines indicate density differing by 10) compared with the model A CMDs plotted in grey (logarithmic scale). The rows of panels from top to bottom show the model CMDs with $\eta = 0.2$ (top row), $\eta = 0.5$ (middle row), and $\eta = 0.9$ (bottom row). The columns of panels from right to left show CMDs sampled at radial distances of 0.9, 2.4, 4.1, and 5.8 kpc from the M33 center.

differences in the metal enrichment history of the models make it possible to break the parameter degeneracy.

However, to constrain galaxy SF parameters, the resolved stellar photometry is necessary. For the CMD analysis we used the HST/ACS WFC stellar photometry data in four fields within the galaxy M33, kindly provided by Benjamin Williams (Williams et al. 2009).

The sizes of areas, used to sample models at different radial distances, are the same as those of areas measured in Williams et al. (2009). To compare the model and observed CMDs we adopt for M33 a distance of 840 kpc, the same extinction for all fields, $A_V = 0.3$, and apply to the model stars Gaussian errors calculated using the relation between photometric errors and magnitude, which was derived from the observed star catalog individually for each field. The extinction for the HST/ACS bands was calculated according to Cardelli, Clayton & Mathis (1989),

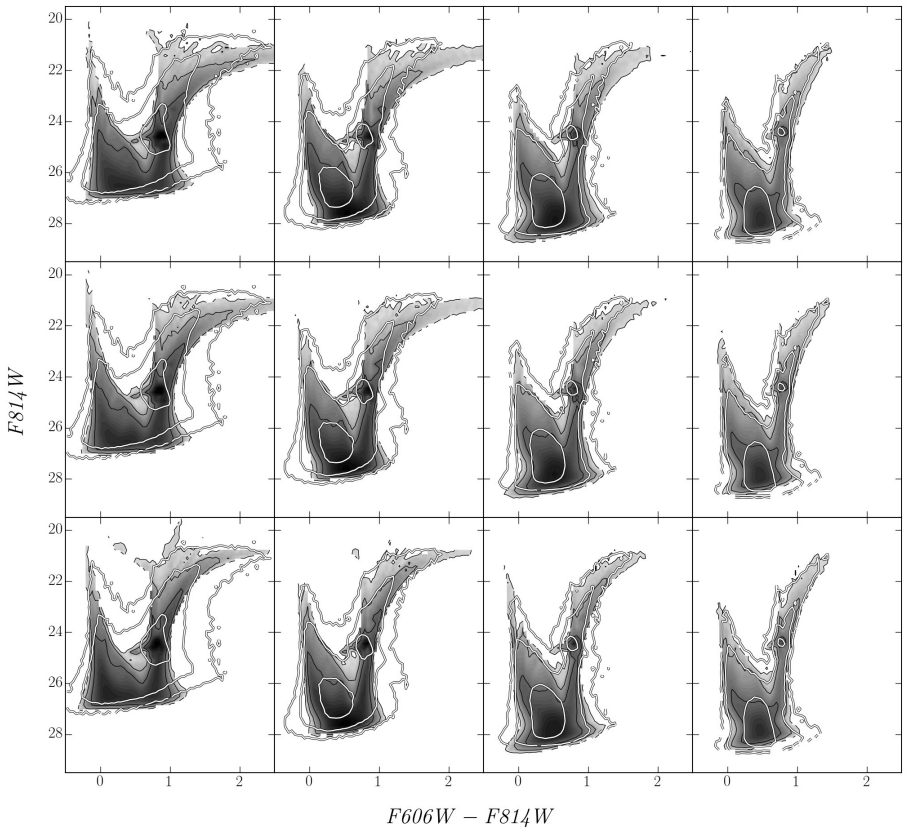

Fig. 3. The same as in Fig. 2, but for the model B.

with $R_V = 3.1$. Note, however, that in estimating the errors we do not take into account the effects of crowded field photometry and differential extinction within the galaxy M33.

In Fig. 2 we plotted CMDs of the model A with different values of the outflow parameter , together with the observational data for M33. The model CMDs with $\eta = 0.2, 0.5, 0.9$ are shown in the top, middle, and bottom rows of panels, respectively. The model CMDs sampled at different distances from the galaxy center, 0.9, 2.4, 4.1, and 5.8 kpc, are shown in the columns of panels from the left to the right, respectively. Fig. 2 shows that CMDs of the model A are incompatible with the M33 data. With $\eta = 0.2, 0.5$, only the CMDs in the outermost fields match the observations. The inner fields display features of clearly too metallic stellar populations in comparison with the observed data. The model CMDs with the highest value of the outflow parameter, $\eta = 0.9$, in the inner fields match the observational data, however, in the outer fields, the models are clearly too metal deficient.

In Fig. 3 we compare, in a similar way, the observations with the model B. In the cases of $\eta = 0.2, 0.5$ we see, again, the CMD features of too metallic stellar populations in the inner fields. However, contrary to the model A, in the case of

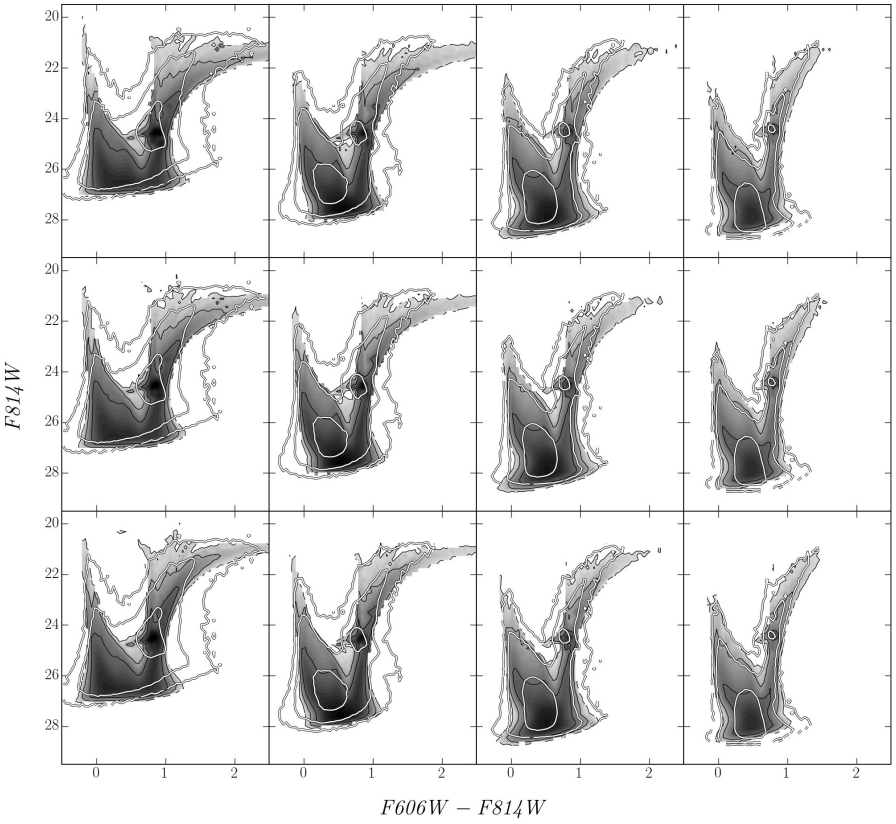

Fig. 4. The same as in Fig. 2, but for the model C.

$\eta = 0.9$ (bottom row of panels), the CMDs of the model B match the observations both in the inner and in the outer fields.

The model C with the lowest value of ϵ is compared with the observations in Fig. 4. The low values of ϵ suppress gas outflow from the galaxy due to relatively low-mass stellar populations forming in the disk. As a result of this effect, even models with highest η values shows too metallic stellar populations throughout the galaxy disk.

5. CONCLUSIONS

We have demonstrated the capability of our improved stochastic 2-D models of galaxy disk evolution to analyze resolved stellar photometry data of the galaxy M33. The method of synthetic CMDs was proved to be a powerful tool to disentangle degeneracies of SF history in the cases when a turn-off of the main sequence is below the detection limit of photometry. The synthetic CMDs help to break parameter degeneracies discussed in our previous paper (Mineikis & Vansevičius 2014a). Therefore, putting together our galaxy disk models, galaxy radial profile observations performed in a wide range of wavelength – from UV to radio, as well as high precision and high resolution stellar photometry observations with

HST, we have demonstrated that degeneracies of the SF history parameters can be resolved.

ACKNOWLEDGMENTS. We are thankful to Dr. Benjamin Williams for providing the HST/ACS WFC stellar photometry catalog of the galaxy M33. This research was partly funded by grant No. MIP-074/2013 from the Research Council of Lithuania.

REFERENCES

Aparicio A., Hidalgo S. L. 2009, AJ, 138, 558
Asplund M., Grevesse N., Sauval A. J., Scott P. 2009, ARA&A, 47, 481
Baumgartner V., Breitschwerdt D. 2013, A&A, 557, AA140
Bressan A., Marigo P., Girardi L. et al. 2012, MNRAS, 427, 127
Cardelli J. A., Clayton G. C., Mathis J. S. 1989, ApJ, 345, 245
Chen Y., Girardi L., Bressan A. et al. 2014, MNRAS, 444, 2525
Corbelli E., Salucci P. 2000, MNRAS, 311, 441
Fakhouri O., Ma C.-P., Boylan-Kolchin M. 2010, MNRAS, 406, 2267
Ferguson A., Irwin M., Chapman S. et al. 2007, *Island Universes – Structure and Evolution of Disk Galaxies*, Springer, p. 239
Gordon K. D., Clayton G. C., Misselt K. A., Landolt A. U., Wolff, M. J. 2003, ApJ, 594, 279
Harris J., Zaritsky D. 2009, AJ, 138, 1243
Heyer M. H., Corbelli E., Schneider S. E., Young J. S. 2004, ApJ, 602, 723
Kroupa P. 2002, Science, 295, 82
Lewis A. R., Dolphin A. E., Dalcanton J. J. et al. 2015, ApJ, 805, 183
Mineikis T., Vansevičius V. 2014a, Baltic Astronomy, 23, 209
Mineikis T., Vansevičius V. 2014b, Baltic Astronomy, 23, 221
Muñoz-Mateos J. C., Gil de Paz A., Boissier S. et al. 2007, ApJ, 658, 1006
Rosolowsky E., Simon J. D. 2008, ApJ, 675, 1213
Rubele S., Girardi L., Kerber L. et al. 2015, MNRAS, 449, 639
Tang J., Bressan A., Rosenfield P. et al. 2014, MNRAS, 445, 4287
Williams B. F., Dalcanton J. J., Dolphin A. E., Holtzman J., Sarajedini A. 2009, ApJL, 695, L15